CHEMICAL ENGINEERING TRANSACTIONS

VOL. 39, 2014

A publication of AIDIC
The Italian Association of Chemical Engineering
www.aidic.it/cet

Guest Editors: Petar Sabev Varbanov, Jiří Jaromír Klemeš, Peng Yen Liew, Jun Yow Yong

ISBN 978-88-95608-30-3; **ISSN** 2283-9216

DOI: 10.3303/CET1439150

Study on Heat Transfer and Pressure Drop Performances of Airfoil-Shaped Printed Circuit Heat Exchanger

Lei Li, Ting Ma, XiangYang Xu, Min Zeng, QiuwWang Wang*

Key Laboratory of Thermal-fluid Science and Engineering, Ministry of Education, Xi'an Jiaotong University, Xi'an, Shaanxi, 710049, P. R. China
wangqw@mail.xjtu.edu.cn

Printed circuit heat exchanger (PCHE) is one of the most promising micro-channel heat exchangers for very high temperature and high pressure conditions. In the present study, PCHE has four channel configurations: straight, zigzag, s-shaped fin and airfoil-shaped fin. In this paper, we investigate the effects of parameters such as Reynolds number, the number of fin rows, fin transverse pitch and longitudinal pitch on the pressure drop and heat transfer by means of CFD code. It is found that the heat transfer and fluid flow approach fully developed conditions when the number of tube rows is greater than 9, and both of the *f* and *Nu* decrease with the increase of fin transverse pitch and longitudinal pitch. The *f* and *Nu* correlations are obtained.

1. Introduction

Compactness and efficiency are used as the essential tools to evaluate a heat exchanger. A High Temperature Gas-cooled Reactor (HTGR) and a Very High Temperature Reactor (VHTR) designs have generated considerable interest in selecting a good heat exchanger for an intermediate heat exchanger (IHX) and a remunerator to utilize high temperature heat for high thermal efficiency and hydrogen production. Therefore, many previous works were focused on the importance of the IHX and selection of the heat exchanger type (Wang et al., 2002).Printed circuit heat exchanger is a promising candidate for compact heat exchangers because it can provide a large amount of heat transfer area in a small volume. Typically, two technologies are applied to manufacture the PCHE: photo-etching and diffusion bonding.
For plate fin heat exchangers, compactness is usually expressed by using the Colburn j factor, given as:

$$j = \frac{D_h}{4L} \mathrm{Pr}^{2/3} N \tag{1}$$

$$N = (T_0 - T_i) / \Delta T_{LMTD} \tag{2}$$

Where: D_h is the hydraulic diameter, L is the length of the heat exchanger, N is the number of thermal units. As shown in Eq(1) and Eq(2) (Hesselgreaves,2001), Reduction of the hydraulic diameter engenders a decreased active length or heat exchanger size at the same Colburn *j* factor, *Pr*, and *N* conditions. By the means of photo-etching, small flow channels are achieved easily. And another technology, diffusion bonding, maintains the parent material strength because of no flux, braze or filler exist in the heat exchanger core. That provides a high capability of corrosion and temperature resistance.

Please cite this article as: Li L., Ma T., Xu X., Zeng M., Wang Q., 2014, Study on heat transfer and pressure drop performances of airfoil-shaped printed circuit heat exchanger, Chemical Engineering Transactions, 39, 895-900 DOI:10.3303/CET1439150

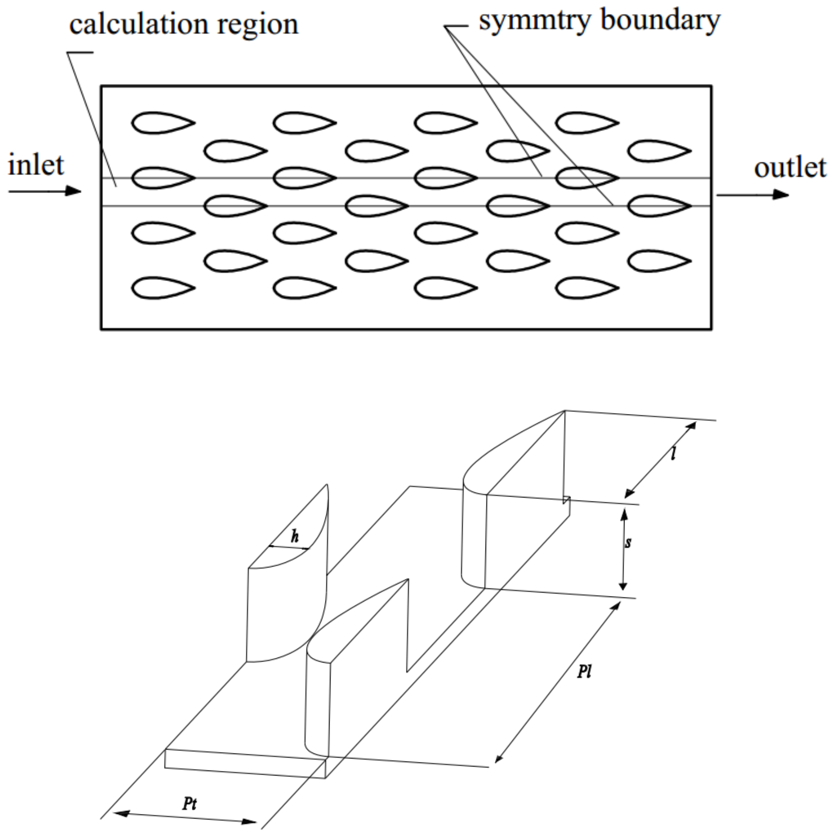

Figure 1: Airfoil-shaped fin

2. Simulation Model

2.1 Physical Model

The airfoil-shaped PCHE with three fin rows is selected as the numerical model, as shown in Figure1. The fin is shaped into NACA airfoil-shape (NACA0021 model), the maximum airfoil thickness is 0.84 mm, the chord length is 4 mm, the height is 1 mm. The simulation is performed in the turbulence region with 3,627<Re<8,161, with the corresponding velocity ranged from 40 m/s to 90 m/s. In this model, the fluid is helium and it is assumed to be steady state, incompressible flow and constant properties.

2.2 Governing Equations and Numerical Methods

Simulation calculations are carried out using the software FLUENT. The governing equations are including continuity, momentum and energy equations:

$$\nabla\left(\rho\vec{U}\right)=0 \tag{3}$$

$$\vec{U}\cdot\nabla\left(\rho\vec{U}\right)=-\nabla p+\nabla\cdot\left(\mu\nabla\vec{U}\right) \tag{4}$$

$$\vec{U}\cdot\nabla\left(\rho c_{\mathrm{p}}T\right)=\nabla\cdot\left(\lambda_{\mathrm{f}}\nabla T\right) \tag{5}$$

In this paper, *Re* is range from 3,687 to 8,161, so turbulence is taken into account by the *k*-*ω* SST model, neglecting the user-defined source terms, equations for the turbulent kinetic energy *k* and the specific heat dissipation rate *ω* can be obtained from Eq(6) and Eq(7), all equations are solved by second-order upwind discretization for convection. The Semi Implicit Method Pressure Linked Equation (SIMPLE) algorithm is used to resolve coupling of velocity and pressure.

$$\frac{\partial}{\partial t}(\rho\kappa)+\frac{\partial}{\partial x_i}(\rho\kappa u_i)=\frac{\partial}{\partial x_i}(\Gamma_\kappa\frac{\partial\kappa}{\partial x_j})+G_\kappa-Y_\kappa \tag{6}$$

$$\frac{\partial}{\partial t}(\rho\omega)+\frac{\partial}{\partial x_i}(\rho\omega u_i)=\frac{\partial}{\partial x_i}(\Gamma_\omega\frac{\partial\omega}{\partial x_j})+G_\omega-Y_\omega+D_\omega \tag{7}$$

The uniform velocity inlet and pressure outlet boundary conditions available in FLUENT are used at the inlets and outlets, the top and bottom boundary conditions are constant temperature at 500 K, the left and right are given a symmetry boundary condition.

In this paper, the Reynolds number, Nusselt number and friction factor characteristics are calculated by Eq(8) to Eq(11).

$$Re=\frac{\rho u_i D_h}{\mu} \tag{8}$$

$$Nu=\frac{hD_h}{\lambda} \tag{9}$$

$$h=\frac{Q}{A\Delta T_{\mathrm{m}}} \tag{10}$$

$$f=\frac{2\Delta p D_h}{\rho u_i^2 L} \tag{11}$$

Where u_i is the inlet velocity, D_h is twice the height of the fin (D_h=2S).

2.3 Grid independence

Before examining the effects of geometrical parameters on the performance of heat transfer and flow friction, it is necessary to adopt an appropriate grid system for computations in turn leading to a correct physical understanding. Only one row fin of the model was studied in the grid independence. Five sets of grid were chosen: 27,786 hexas, 38,500 hexas, 54,378 hexas, 89,433 hexas and 141,588 hexas, and the computations are performed for a case with Reynolds number being 3,267. The results are shown in Fig. 2(a). Comparing the results on the finest grid with the third grid, the deviations of Nu and f are 0.14 % and 0.33 %.Because the structure of the model is similar to the tube-fin heat exchanger. The method is performed to examine the applicability by comparing with experiment (Tang et al., 2009) and the comparisons are shown in Figure 2(b). The deviation of Nusselt number using *k-ω* SST method between numerical and experimental results is less than 8.9 % and the deviation of *f* factor is less than 11.5 %.According to the above comparison, the method is reliable.

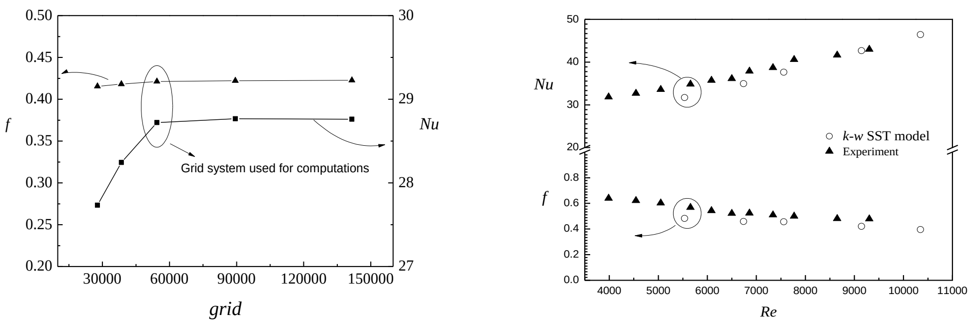

Figure 2: The results of grid independence tests

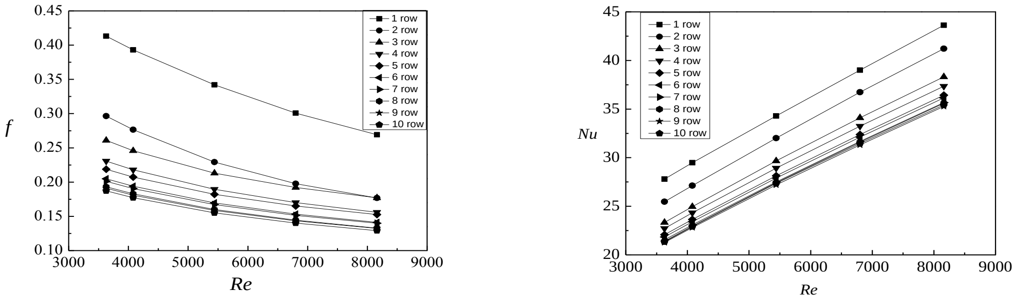

Figure 3: Effect of Re and fin rows number on f and Nu (a) Effect of Re and fin rows number on f (b) Effect of Re and fin rows number on Nu

3. Result and Discussion

3.1 Fin rows

The numerical results of *Nu* and *f* with different *Re* and fin rows number are shown in Figure 3. With the increase of *Re* number, the *Nu* number increases while *f* decreases. It also can be seen that the *Nu* and *f* decrease with the increasing of the fin row, that because the enhanced phenomenon at the inlet region. But the *Nu* and *f* are almost identical when the row number is larger than 9. So there is no need to compute the model with more rows.

3.2 Fin transverse pitch and longitudinal pitch

The numerical results of *Nu* and f with different fin transverse pitch and longitudinal pitch are shown in Figure 4. The transverse pitch are 1.5 mm, 1.6 mm, 1.7 mm, 1.8 mm and 1.9 mm; the longitudinal pitch are 4 mm, 5 mm, 6 mm, 7 mm and 8 mm. The characteristics may be summarized as follows. Both *Nu* and *f* decrease with the increasing of transverse pitch, that because if it has a same velocity at the inlet, the flow channel with a larger transverse pitch has a smaller velocity at the minimum free flow cross-section, then the flow turbulence is reduced, witch lead to a small Nusselt number and friction factor. And the *Nu* number and *f* decrease with the increasing of the longitudinal pitch, that is because, when the channel has larger longitudinal pitch, it can create a larger flow area that will decrease the flow resistance. From Figure 4, it can be seen the transvers pitch has more effect on heat transfer and pressure drop than the longitudinal pitch, which is similar to Xie et al. (2009).

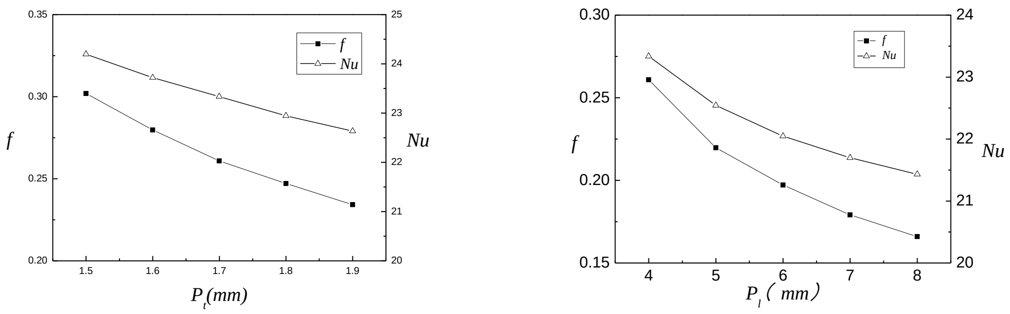

Figure 4: Effect of transverse and longitudinal pitch number on f and Nu (a) Transverse pitch (P_t), (b) Longitudinal pitch (P_l)

3.3 Multiple correlations

Based on the principle of similarity theory, the present data can be extrapolated or interpolated to other conditions by established correlations. For this reason, it is useful to try to obtain suitable correlations. The forms for correlations may be diversified, however, in order to reduce the difficulty involved in correlating the data and to refer to previous forms, the following forms are assumed:

$$f = C_0 N^{C_1} \mathrm{Re}^{C_2} (\frac{h}{P_t})^{C_3} (\frac{l}{P_l})^{C_4} \tag{12}$$

$$Nu = C_0 N^{C_1} \mathrm{Re}^{C_2} (\frac{h}{P_t})^{C_3} (\frac{l}{P_l})^{C_4} \tag{13}$$

Base on the foregoing numerical data and 1stopt15PRO code. The five coefficients are determined. Then the correlations become Eq(10) and Eq(11) (3,627 <*Re*<8,161):

$$f = 47.00654 N^{-0.35035} \mathrm{Re}^{-0.49475} (\frac{h}{P_t})^{1.033682} (\frac{l}{P_l})^{0.726493} \tag{14}$$

$$Nu = 0.20756 N^{-0.10518} \mathrm{Re}^{0.615001} (\frac{h}{P_t})^{0.268556} (\frac{l}{P_l})^{0.155274} \tag{15}$$

It is again noted that the valid range for the parameters. The *Re* ranged from 3,627 to 8,161; the transverse pitch ranged from 1.5 mm to 1.9 mm; the longitudinal pitch ranged from 4 mm to 9 mm, the predicted results and numerical data are compared as shown in Figure 5. Almost deviations are within 5 %, which indicate that the heat transfer and pressure drop correlations are of sufficient accuracy.

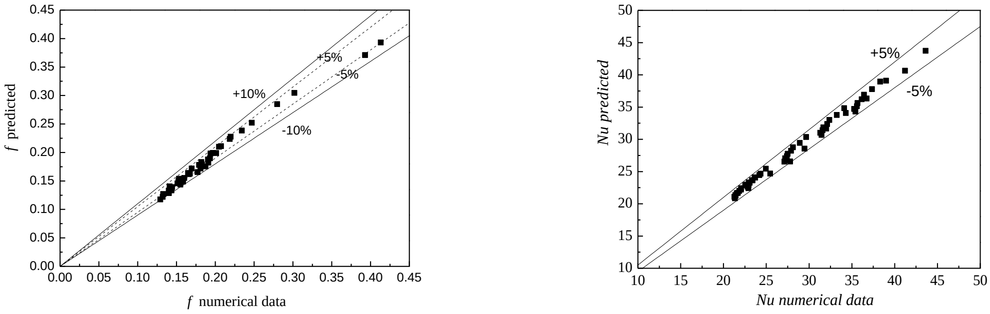

Figure 5: Comparison between predicted results and numerical data

4. Conclusions

3D-computations on fluid-side turbulence flow and heat transfer of air-foil shaped fin heat exchangers are conducted to reveal the effects of Reynolds number, the number of tube rows, fin transvers pitch and longitudinal pitch on the overall Nusselt number and friction factor. Base on the numerical results, the heat transfer and flow friction correlations are established. Few experiments have been done of PCHE with air-foil shaped fin, but that are necessary to verify the simulation results and study on the new configuration heat exchanger. And the major findings are summarized as follows:

1) With the increase of *Re* number, the *Nu* number increases while *f* decreases, the *Nu* and *f* are almost identical to those of rows number being 9 when the rows number larger than 9.
2) Both *Nu* and *f* are decrease with the increase of transverse pitch, as well as longitudinal pitch. That is because, when the channel has larger transverse pitch or longitudinal pitch, it can create a larger flow area that will decrease the flow resistance.
3) Multiple correlations of the *Nu* number and *f* factor have been established, and the correlations are of sufficient accuracy

Acknowledgement

This work is financially supported by the International Cooperation and Exchanges Project of NSFC of China (Grant No. 51120165002), National Natural Science Foundation of China (Grant No. 51025623, 51306139) and Specialized Research Fund for the Doctoral Program of Higher Education of China (Grant No. 20130201120061).

References

Hesselgreaves J.E., 2001, Compact Heat Exchanger, Selection, Design and Operation (first edition), Pergamon/Elsevier, Oxford, UK.

Kim D.E., Kim M.H., Cha J.E., Kim S.O., 2008, Numerical investigation on thermal–hydraulic performance of new printed circuit heat exchanger model. Nuclear Engineering and Design, 238, 3269–3276.

Tsuzuki N., Kato Y., Ishizuka T., 2005, High performance printed circuit heat exchanger, Proceedings of Heat SET 2005, Heat Transfer in Components and Systems for Sustainable Energy Technologies, Grenoble, France, April 5–7.

Ngo T.L., Kato Y., Nikitin K., Ishizuka T., 2007, Heat transfer and pressure drop correlations of micro channel heat exchangers with S-shaped and zigzag fins for carbon dioxide cycles. Experimental Thermal and Fluid Science, 32(2): 560-570.

Tang L.H, Zeng M., Xie G.N., Wang Q.W., 2009, Fin Pattern Effects on Air-Side Heat Transfer and Friction Characteristics of Fin-and-Tube Heat Exchangers with Large Number of Large-Diameter Tube Rows. Heat Transfer Engineering, 30(3):171-180.

Kim I.H., No H.C., Lee J.I., Jeon B.G., 2009, Thermal hydraulic performance analysis of the printed circuit heat exchanger using a helium test facility and CFD simulations. Nuclear Engineering and Design, 239, 2399–2408.

Tao W.Q., 2001, Numerical Heat Transfer (second edition). 1-5.

Xie G.N., Wang Q.W., Sunden B., 2009, Parametric study and multiple correlations on air-side heat transfer and friction characteristics of fin-and-tube heat exchangers with large number of large-diameter tube rows. Applied Thermal Engineering 29, 1–16.

Mylavarapu S., 2008, Development of compact heat exchangers for very high-temperature gas-cooled reactors. Columbus: Ohio State University, USA.

Ngo T.L., Kato Y., Nikitin K., Tsuzuki N., 2006, New printed circuit heat exchanger with S-shaped fins for hot water supplier. Experimental Thermal and Fluid Science, 30(8): 811-819.